APPLICATION OF BOND GRAPH TO PERMANENT MAGNET BRUSHLESS DC MOTOR DRIVE

V.SOWMYA SREE, N. RAVI SANKAR REDDY
Department of EEE, G. Pulla Reddy Engineering College (Autonomous)
Kurnool, Andhra Pradesh, India.
sowmya.sree14@gmail.com, netapallyravi@gmail.com

Abstract—

This paper presents a study of BLDC motor drive modelling using classical method and bond graph theory. System equations are generated by using a step-by-step procedure from bond graph theory. Bond Graph method is rapidly developing to promote a new methodology of modelling and simulation of electrical systems that suits for multi-domain systems effectively. The dynamic behaviour of the BLDC motor drive has been studied from the simulation results that are obtained by using MATLAB/SIMULINK software package.

Key words— *Bond graph,BLDC motor ,MATLAB/SIMULINK*

1. Introduction

The Brushless DC (BLDC) motor is being used in different applications such as industrial automation, automotive, aerospace, instrumentation and appliances since 1970's and is considered as the optimal choice for long-term applications. It is a high performance motor providing large amounts of torque over a wide speed range. BLDC motors do not have brushes and requires less maintenance. Based on the shape of back-emf waveforms [6], the BLDC motor drives are classified into trapezoidal and sinusoidal type back-emf BLDC motors.

Bond graph is a domain-independent graphical description of physical systems dynamic behavior. In 1959, Prof. H.M.Paynter invented the idea of portraying systems in terms of power bonds, connecting the elements of the physical system to the junction structures. This power exchange portray of a system is called Bond Graph which is both power and information oriented. The idea was further developed by Karnopp and Rosenberg such that it could be used in practice. [1]

By this approach, a physical system can be represented by symbols and lines, identifying the power flow paths. The lumped parameter elements resistance, capacitance and inductance are interconnected in an energy conserving way by bonds and junctions resulting in a network structure. The flow of energy between two elements is always characterized by two generalized conjugated variables e (effort) and f (flow), of which the product is power P. [2, 4]

$$P = e\,f$$

In this technique, power flow is represented by a half bond. Every bond is associated with two variables, effort and flow and the causality indication.

A three phase, 4-pole, Y connected trapezoidal back-EMF type BLDC motor is modeled in two methods. The first method is using the mathematical equations derived from the equivalent circuit of the BLDC motor drive. The second approach is developing a bond-graph model of equivalent circuit of the BLDC motor drive and deriving state-space equation from bond-graph theory.

2. Bond Graph Standard Elements

2.1 Basic 1-Port Elements

A 1-port element has a single pair of effort and flow variables. Ports are classified as passive ports and active ports. The passive ports are idealized elements because they contain no power sources. The inductor, capacitor, and resistor are classified as passive elements. [5]

2.1.1 R-Element:

The R-element is expressed as generalized friction and contains effort and flow variables. It controls dissipation of power.

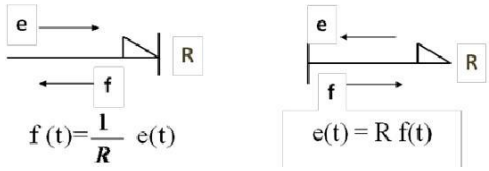

Fig.1. R-bond

2.1.2 L-Element:

The inertia L-element expresses all effects containing effort and flow variables. It provides storage for power

that includes inductance and inertia.

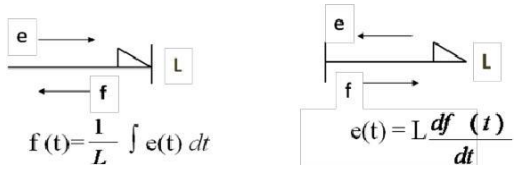

Fig.2. L-bond

2.1.3 C-Element:

The capacitance C-element expresses all effects containing effort and flow variables. It provides storage for power including condensers, springs and accumulators.

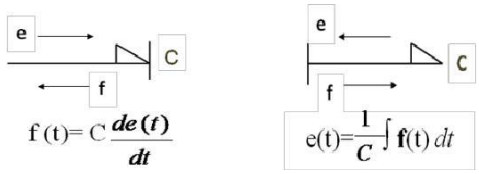

Fig.3. C-bond

2.1.4 Effort & Flow Sources:

The active ports responds to the source.

Fig. 4. SE & SF-bonds

2.2 Basic 2-Port Elements

Transformer and Gyrator are the two-port elements. The bond graph symbols for these elements are TF and GY, respectively. As the name suggests, two bonds are attached to these elements. [5]

2.2.1 TF-Element:

The transformer transforms either a flow into another flow or an effort into another effort. 'm' is the transformation ratio.

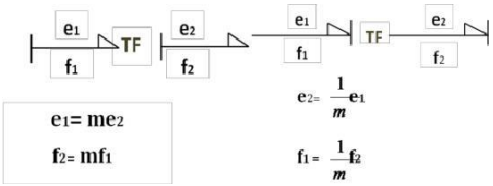

Fig.5. TF-bond

2.2.2 GY-Element:

The gyrator transforms a flow into an effort or an effort into a flow. 'r' is the gyrator ratio.

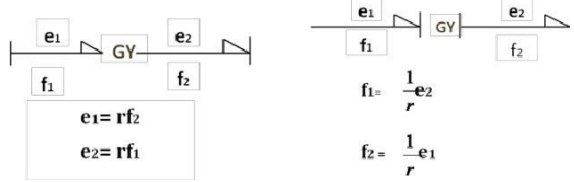

Fig.6. GY-bond

2.3 Multi-Port Elements

These include 0-junction and 1-junction. [5]

2.3.1 1-Junction:

The flows on the bonds attached to a 1-junction are equal and the algebraic sum of the efforts is zero. For series connections 1-junctions are used.

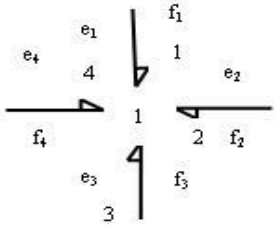

$$e_1f_1 + e_2f_2 + e_3f_3 + e_4f_4 = 0$$

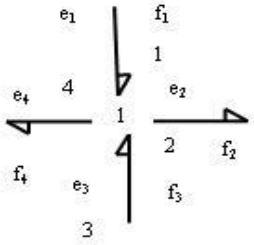

$$e_1f_1 - e_2f_2 + e_3f_3 - e_4f_4 = 0$$

Fig.7. 1-Junction

2.3.2 0-Junction:

The efforts on the bonds attached to a 0-junction are equal and the algebraic sum of the flows is zero. For parallel connections 0-junctions are used.

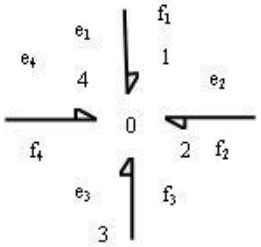

$$e_1f_1 + e_2f_2 + e_3f_3 + e_4f_4 = 0$$

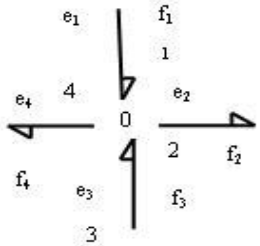

$$e_1f_1 - e_2f_2 + e_3f_3 - e_4f_4 = 0$$

Fig.8. 0-Junction

3. Modelling of BLDC Motor

Fig 9 shows the equivalent circuit of BLDC motor drive. The following are the assumptions made for modelling:

• Stator resistance and self inductance of all phases are equal and constant and mutual inductance is taken zero.
• Hysteresis and eddy current losses are eliminated.
• All semiconductor switches are ideal.

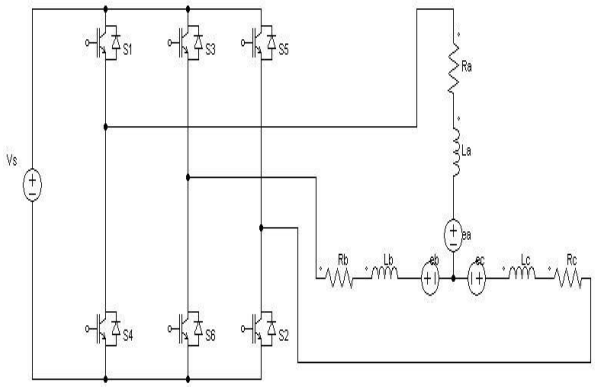

Fig.9. BLDC motor drive

3.1 Classical Approach:

The three phase voltages are given by

$$\left.\begin{aligned} Va &= Ri_a + L\frac{di_a}{dt} + Ea \\ Vb &= Ri_b + L\frac{di_b}{dt} + Eb \\ Vc &= Ri_c + L\frac{di_c}{dt} + Ec \end{aligned}\right\} \quad (1)$$

The three phases back-emf are given by

$$\left.\begin{aligned} Ea &= Ke * \omega m * Fa(\theta) \\ Eb &= Ke * \omega m * Fa\left(\theta - \frac{2\pi}{3}\right) = Ke * \omega m * Fb(\theta) \\ Ec &= Ke * \omega m * Fa\left(\theta + \frac{2\pi}{3}\right) = Ke * \omega m * Fc(\theta) \end{aligned}\right\} \quad (2)$$

The trapezoidal back-emf function F(Θ) is given by

$$Fa(\theta) = \begin{cases} 1 & 0 \le \theta \le 2\pi/3 \\ 1 - \frac{6}{\pi}(\theta - 2\pi/3) & 2\pi/3 \le \theta \le \pi \\ -1 & \pi \le \theta \le 2\pi/3 \\ -1 + \frac{6}{\pi}(\theta - 5\pi/3) & 5\pi/3 \le \theta \le 2\pi \end{cases} \quad (3)$$

The electromagnetic torque equation is given by

$$Te = \frac{Eaia + Ebib + Ecic}{\omega m} \quad (4)$$

The electromagnetic torque generated by the motor is also proportional to the torque constant (K_t) and product of current with electrical rotor position.

$$Te = Kt * ia * Fa(\theta) + Kt * ib * Fb(\theta) + Kt * ic * Fc(\theta) \quad (5)$$

The equation of motor for simple system is

$$Te = B\omega m + J\frac{d\omega m}{dt} + Tl \quad (6)$$

where, T_l is the load torque, J is moment of inertia and B is the damping constant.

$$\frac{d\theta}{dt} = \frac{P}{2} * \omega m \quad (7)$$

3.2 Bond Graph Approach :

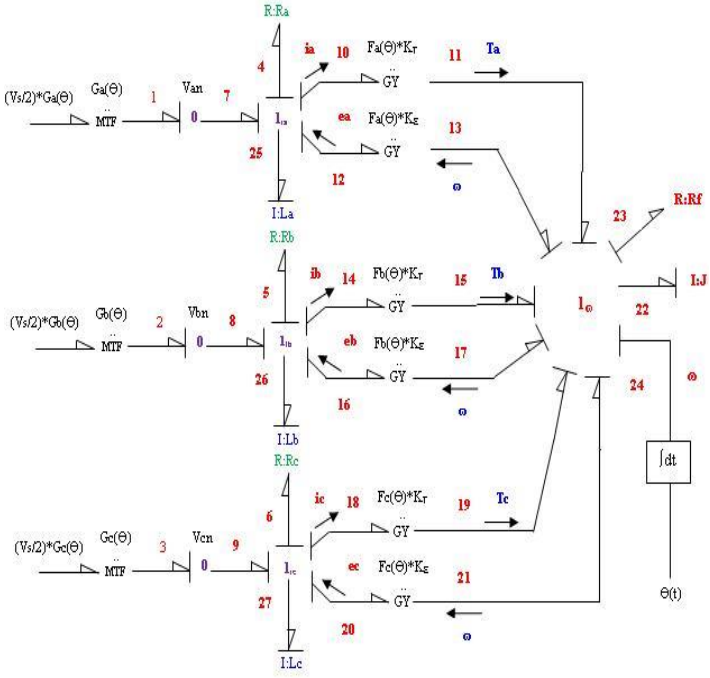

Fig.10. Bond Graph Model of BLDC motor drive

The following step-by-step procedure [3] is required to generate system equations.

i) The system variables and sources given to the system by all the elements present in system are as follows:

1. Element La gives the flow f_{25} = p1/La
2. Element Lb gives the flow f_{26} = p2/Lb
3. Element Lc gives the flow f_{27} = p3/Lc
4. Rotational element J gives the flow $f2_{22}$ = p4/J
5. Element Ra gives the effort e_4 = Ra*f_4
6. Element Rb gives the effort e_5 = Rb*f_5
7. Element Rc gives the effort e_6 = Rc*f_6
8. Element Rf gives the effort e_{23} = Rf*f_{23}

Where p1,p2,p3 are the electrical momentums and p4 is the angular momentum.
e's and f's are efforts and flows of system respectively.

ii) The efforts and flows given to the storage elements from the system with integral causality are as follows:

1. To La, system gives the effort e_{25}= dp1/dt
2. To Lb, system gives the effort e_{26}= dp2/dt
3. To Lc, system gives the effort e_{27}= dp3/dt
4. To J, system gives the flow f_{24}= dq24/dt

Applying KVL and KCL to 0- and 1- junctions present in the system, the modelling equations for BLDC motor are given as:

a) $e_{25} = e_7 - e_4 - e_{12}$
b) $e_{26} = e_8 - e_5 - e_{16}$
c) $e_{27} = e_9 - e_6 - e_{20}$
d) $f_4 = f_7 = f_{10} = f_{12} = f_{25}$
e) $f_5 = f_8 = f_{14} = f_{16} = f_{26}$
f) $f_6 = f_9 = f_{18} = f_{20} = f_{27}$

The equations for three-phase torques, back-emfs and currents are given as follows:

$$\begin{aligned} Ta &= e_{11} = F_a(\theta) * K_t * f_{10} \\ Tb &= e_{15} = F_b(\theta) * K_t * f_{14} \\ Tc &= e_{19} = F_c(\theta) * K_t * f_{18} \end{aligned} \quad (8)$$

$$\begin{aligned} Ea &= e_{12} = F_a(\theta) * K_e * f_{13} \\ Eb &= e_{16} = F_b(\theta) * K_e * f_{17} \\ Ec &= e_{20} = F_c(\theta) * K_e * f_{21} \end{aligned} \quad (9)$$

$$\begin{aligned} ia &= f_{10} \\ ib &= f_{14} \\ ic &= f_{18} \end{aligned} \quad (10)$$

Angular displacement is given by p4/J in radians.

The state-space model is defined by all the above equations:

$$dX/dt = AX + BU \quad (11)$$

$$A = \begin{bmatrix} -Ra/La & 0 & 0 & -Fa(\theta) * Ke/J & 0 \\ 0 & -Rb/Lb & 0 & -Fb(\theta) * Ke/J & 0 \\ 0 & 0 & -Rc/Lc & -Fc(\theta) * Ke/J & 0 \\ Fa(\theta) * Kt/La & Fb(\theta) * Kt/La & Fc(\theta) * Kt/La & -Rf/J & 0 \\ 0 & 0 & 0 & 1/J & 0 \end{bmatrix}$$

$$X = \begin{bmatrix} p1 \\ p2 \\ p3 \\ p4 \\ q24 \end{bmatrix} \qquad B = \begin{bmatrix} Ga(\theta) \\ Gb(\theta) \\ Gc(\theta) \\ 0 \\ 0 \end{bmatrix} \qquad U = \frac{Vs}{2}$$

In this approach, the state-variables are obtained from the state-space model [8]. The three-phase currents, back-emfs, speed, torque and angular displacement are directly obtained from the state-space variables.

The modulated transformer MTF has a transformation ratio equal to a variable value that is provided by the input signal. Here the rotor position theta generated from the input signal decides the transformation ratio of MTF. For a modulated transformer, effort causality on the incoming bond results in flow causality on the outgoing bond.

4. Generation of Inverter Pulses and Trapezoidal Back-emf Functions

A program [9] is written to generate the inverter pulses and Trapezoidal Back-emf functions with 120^0 phase shift as a function of rotor position.

- A three-phase sinusoidal input with 120^0 phase displacement is generated.
- A 3-phase to 2-phase conversion is done using d-q axis theory.
- The rotor position theta is defined from the 2-phase voltages.
- The pulses are generated in terms of input voltage source depending upon rotor position.
- The conduction period is 120^0 with 60^0 commutation intervals.

5. Results and Discussions

MATLAB/SIMULINK software package is used for the modelling and simulation of the BLDC motor with a time-period of 0.2seconds.

The ratings are DC voltage source = 24 V, No-load current = 8.6A, Moment of inertia = 0.00007 kg-m^2, Back-emf constant = 0.058823 V/rad/sec, Torque constant = 0.05325 N-m/A, Stator resistance = 1.0 ohms, Stator inductance = 0.00005H and Damping constant = 0.000005 N-m/rad/sec.

Figure.11 shows the simulink of mathematical model [9] of equivalent circuit of BLDC motor drive

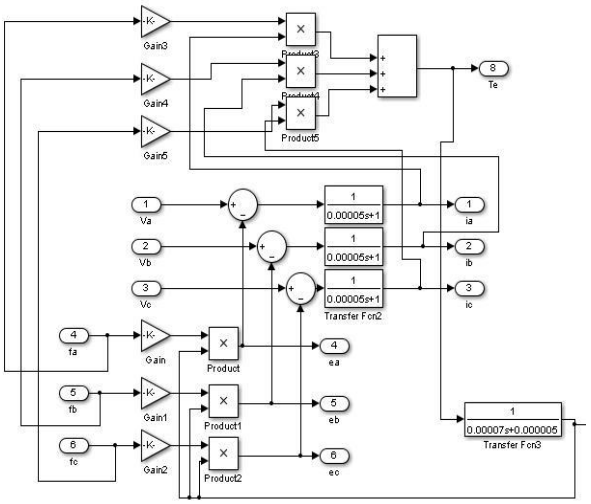

Fig.11. Block diagram of BLDC mathematical model

The three-phase currents are obtained as shown in fig.12.

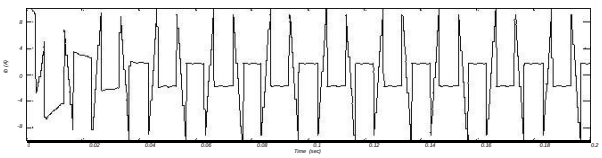

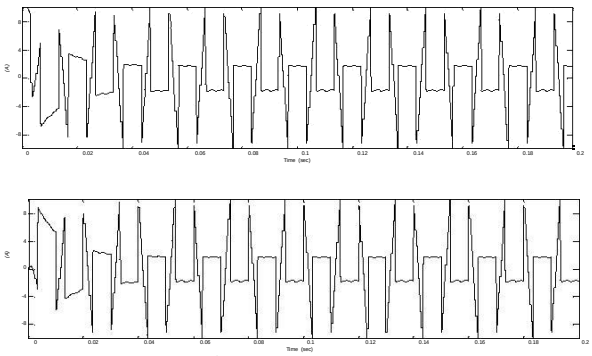

Fig.12. 3-phase currents of BLDC motor using mathematical model

The three-phase back-emf waveforms are as shown in fig.13.

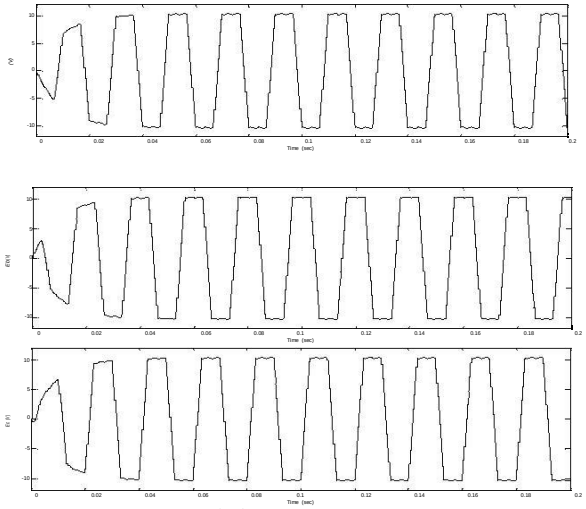

Fig.13. 3-phases back-emf of BLDC motor using mathematical model

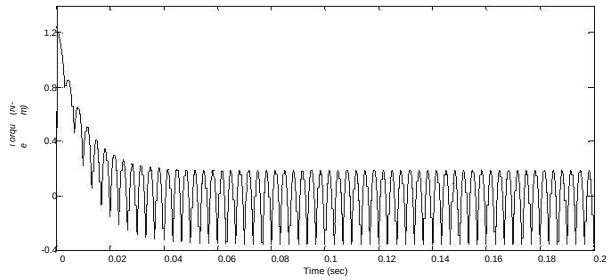

Fig.14. Torque plot of BLDC motor using mathematical model

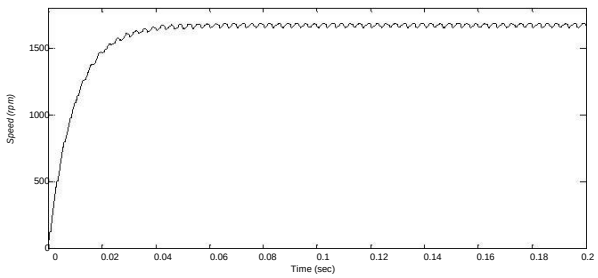

Fig.15. Angular Speed of BLDC motor using mathematical model

The bond graph models are implemented in the form of causality arguments and state-space equations. The simulation time is taken as 0.2seconds.

Fig.16 shows the inverter pulses Ga(θ) , Gb(θ) , Gc(θ)

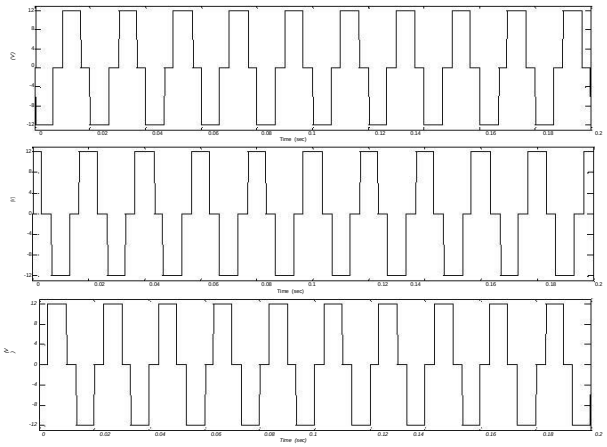

Fig.16. Pulse Pattern of BLDC motor drive

Fig.17 shows the 3-phase Trapezoidal back-emf functions.

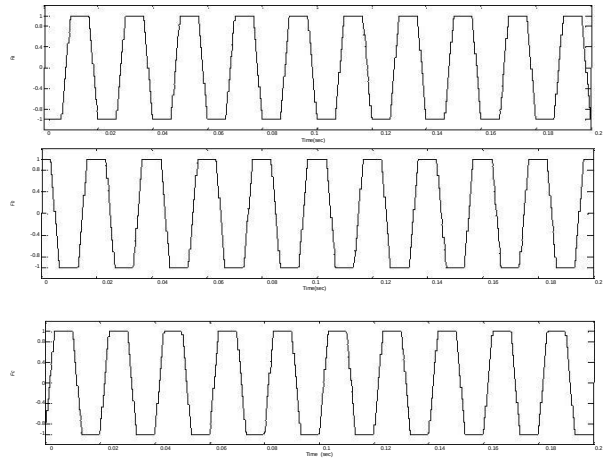

Fig.17. Trapezoidal back-emf functions of BLDC motor drive

Fig.18 shows the three-phase currents of BLDC motor drive.

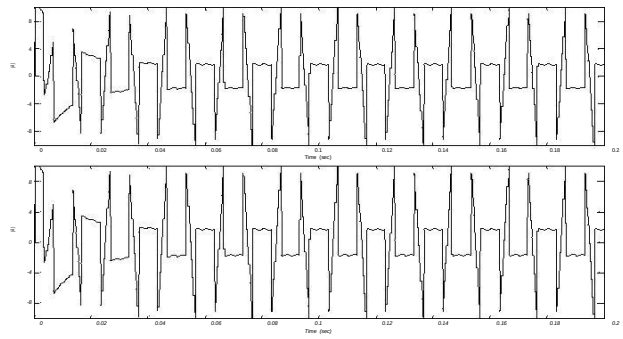

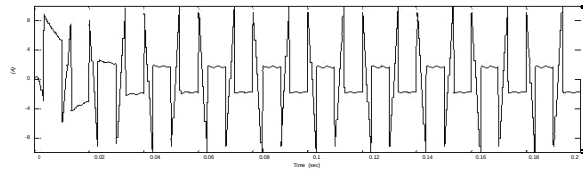

Fig.18. Three-phase currents of BLDC motor drive using Bond Graph theory

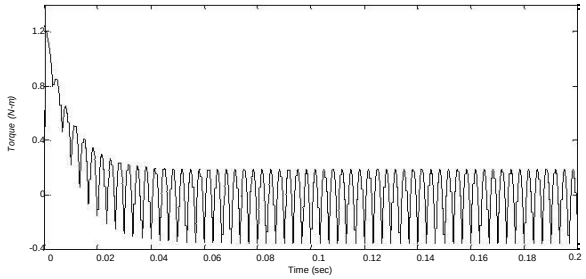

Fig.19. Torque vs. time plot of BLDC motor drive using Bond Graph theory

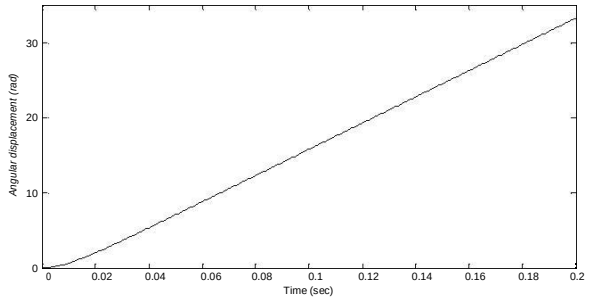

Fig.20. Angular Displacement plot of BLDC motor drive using Bond Graph theory

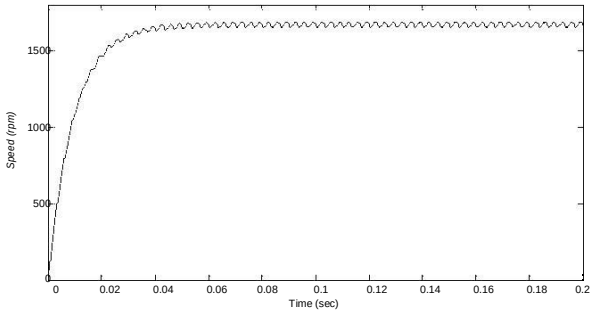

Fig.21. Angular speed of BLDC motor drive using Bond Graph theory

6. Conclusions

The number of computations is reduced by the bond graph approach. No Hall-effect sensors are used for commutation purpose. For any electrical equivalent circuit, it is easy to develop state space equations by this bond graph method. From the results, it is observed that the currents, back-emfs, speed and torque obtained for BLDC motor drive in both classical and bond graph approach are same with less number of computations in bond graph approach.

From fig.15, it is observed currents have quasi-square shape with variations at the commutation points. The starting value is high and reaches a no-load value of around 8.2Amps.

From fig.17, it is observed that the back-emfs are trapezoidal in shape. The linear relation between rotor torque and currents is obtained from this trapezoidal back-emfs.

From fig.19, it is seen that the torque is produced by the rotor continuously

From fig.20 it is observed that there is continuous increase in the angular displacement. It is also observed that there is non-linearity at the starting because of motor acceleration.

Linear matrix inequalities (LMIs) optimization [10] is used for developing two state feedback sliding mode control schemes for position control of brushless DC motor drives to reduce harmonics obtained in the proposed open loop system. A state-space model is developed in this technique [12] for robust sliding mode control but is time consuming which is a closed loop control.

References:

[1] Amod C. Umarikar, Tusharkant Mishra And L. Umanand , "*Bond Graph Simulation And Symbolic Extraction Toolbox In Matlab/Simulink*", J. Indian Inst. Sci., Jan.–Feb. 2006, **86**, 45–68.

[2] Anand Vaz, PS.S.Dhami and PSandesh Trivedi, "*Bond Graph Modeling and Simulation of Three phase PM BLDC Motor*", 14th National Conference on Machines and Mechanisms (NaCoMM09), NIT, Durgapur, India, December 17-18, 2009.

[3] José Antonio Calvo, Carolina Álvarez-Caldas and José Luis San Román, "*Analysis of Dynamic Systems Using Bond Graph Method Through SIMULINK*" Sapin.

[4] Samantaray, www.bondgraphs.com, 2001, pg.1-25.
Jan F. Broenink, "*Introduction to Physical Systems Modelling with Bond Graphs*" University of Twente, Dept EE, Control Laboratory.

[5] Amalendu Mukherjee, Arun Kumar Samantaray, Ranjith karmakar," *Bond Graph In Modeling, Simulation And Fault Identification"*I.K.Publishers.

[6] Padmaraja Yedamale, "*Brushless DC (BLDC) Motor Fundamentals",* Application note 885, Microchip Technology Inc., Chandler, AZ, 2003.

[7] Dr. Jamal A. Mohammed, "*Modeling and Dynamic Performance Analysis of PMBLDC Motor*" Eng. & Tech Journal, Vol.28, No.20, 2010.

[8] B.N.Kartheek, P.S.D.M.Chandana, S.Niveditha, "*An Optimized Code for Space Vector PWM for A Two Level Voltage Source Inverter*" International Journal of Science and Modern Engineering (IJISME) ISSN: 2319-6386, Volume-1, Issue-5, April 2013.

[9] A. Tashakori, *Member IAENG*, M. Ektesabi, *Member IAENG* and N. Hosseinzadeh, "*Modeling of BLDC Motor with Ideal Back-EMF for Automotive Applications*" Proceedings of the World Congress on Engineering Vol II, WCE 2011, July 6 - 8, 2011, London, U.K.

[10] H.M.Soliman, Ehab.H.E.Bayoumi, and M.Soliman, "Robust Guaranteed-Cost Sliding Mode Control of Brushless DC motor: An LMI Approach". International Journal of Modelling, Identification and Control (IJMIC), Vol 17, No. 3, pp.251-260, 2012.

[11] M.Awadallah, E.H.E.Bayoumi and H.M.Soliman, "Adaptive Deadbeat Controllers for BLDC Drives using PSO and ANFIS Techniques", Journal of Electrical Engineering, Vol 60, No. 1, pp. 3-11, 2009.

[12] H.M. Soliman, E.H.E.Bayoumi, M.Soliman "LMI-based sliding mode control for brushless DC motor drives", Proc. IMechE Part I: J. Systems and Control Engineering, Vol. 223, No. 8, pp.1035-1043, 2009.